MRI and 18FET-PET predict survival benefit from bevacizumab plus radiotherapy in patients with IDH wild-type glioblastoma: results from the randomized ARTE trial

Wirsching, Hans-Georg ; Roelcke, Ulrich ; Weller, Jonathan ; Hundsberger, Thomas ; Hottinger, Andreas Felix ; von Moos, Roger ; Caparrotti, Francesca ; Conen, Katrin ; Remonda, Luca ; Roth, Patrick ; Ochsenbein, Adrian F ; Tabatabai, Ghazaleh ; Weller, Michael

Abstract: PURPOSE: To explore a prognostic or predictive role of magnetic resonance imaging (MRI) and O-(2-^{18}F-fluoroethyl)-L-tyrosine (^{18}FET) positron emission tomography (PET) parameters for outcome in the randomized multi-center trial ARTE that compared bevacizumab plus radiotherapy with radiotherpay alone in elderly patients with glioblastoma. EXPERIMENTAL DESIGN: Patients with isocitrate dehydrogenase wild-type glioblastoma aged 65 years or older were included in this post-hoc analysis. Tumor volumetric and apparent diffusion coefficient (ADC) analyses of serial MRI scans from 67 patients and serial ^{18}FET-PET tumor-to-brain intensity ratios (TBR) from 31 patients were analyzed blinded for treatment arm and outcome. Multivariate Cox regression analysis was done to account for established prognostic factors and treatment arm. RESULTS: Overall survival benefit from bevacizumab plus radiotherapy compared to radiotherapy alone was observed for larger pre-treatment MRI contrast-enhancing tumor (hazard ratio [HR] per cm^3 0.94, 95% confidence interval [CI] 0.89-0.99) and for higher ADC (HR 0.18, CI 0.05-0.66). Higher ^{18}FET-TBR on pre-treatment PET scans was associated with inferior overall survival in both arms. Response assessed by standard MRI-based RANO criteria was associated with overall survival in the bevacizumab plus radiotherapy arm by trend only (p=0.09). High ^{18}FET-TBR of non-contrast-enhancing tumor portions during bevacizumab therapy was associated with inferior overall survival on multivariate analysis (HR 5.97, CI 1.16-30.8). CONCLUSION: Large pre-treatment contrast-enhancing tumor mass and higher ADC identify patients who may experience a survival benefit from bevacizumab plus radiotherapy. Persistent ^{18}FET-PET signal of no longer contrast-enhancing tumor after concomitant bevacizumab plus radiotherapy suggests pseudoresponse and predicts poor outcome. TRIAL REGISTRATION: NCT01443676.

DOI: https://doi.org/10.1158/1078-0432.CCR-20-2096

benefit from bevacizumab plus radiotherapy in patients with IDH wild-type glioblastoma: results from the randomized ARTE trial. Clinical Cancer Research, 27(1):179-188.
DOI: https://doi.org/10.1158/1078-0432.CCR-20-2096

MRI and ^{18}FET-PET predict survival benefit from bevacizumab plus radiotherapy in IDH wild-type glioblastoma: the randomized ARTE trial

Hans-Georg Wirsching,[1] Ulrich Roelcke,[2] Jonathan Weller,[1] Thomas Hundsberger,[3] Andreas F. Hottinger,[4] Roger von Moos,[5] Francesca Caparrotti,[6] Katrin Conen,[7] Luca Remonda,[8] Patrick Roth,[1] Adrian Ochsenbein,[9] Ghazaleh Tabatabai,[1] and Michael Weller[1]

[1] Department of Neurology, University Hospital and University of Zurich, Zurich, Switzerland
[2] Department of Neurology, Cantonal Hospital Aarau, Aarau, Switzerland
[3] Department of Neurology, Cantonal Hospital St. Gallen, St. Gallen, Switzerland
[4] Departments of Clinical Neurosciences and Medical Oncology, University Hospital Lausanne, Lausanne, Switzerland
[5] Department of Medical Oncology, Cantonal Hospital Graubuenden, Chur, Switzerland
[6] Department of Radiation Oncology, University Hospital Geneva, Geneva, Switzerland
[7] Department of Medical Oncology, University Hospital Basel, Basel, Switzerland
[8] Department of Neuroradiology, Cantonal Hospital Aarau, Aarau, Switzerland
[9] Department of Medical Oncology, Inselspital, Berne University Hospital, University of Berne, Berne, Switzerland

Corresponding author: Hans-Georg Wirsching, MD, Department of Neurology, University Hospital and University of Zurich, Frauenklinikstrasse 26, CH-8091 Zurich, Switzerland, Phone: +41 44 255 5500, Fax: +41 44 255 3091, Email: hans-georg.wirsching@usz.ch

Running Title: MRI/PET and benefit from BEV plus RT in glioblastoma

Keywords: Anti-angiogenesis, glioma, imaging, outcome

Funding: The study was supported by a grant from F. Hoffmann-La Roche. HGW was supported by a grant from the University Hospital Zurich.

Conflicts of interest: HGW, GT, PR and MW received honoraria for advisory boards from F. Hoffmann-La Roche.

Authorship: HGW, UR and MW conceptualized the work, UR and JW analyzed imaging data, all authors contributed to data acquisition, revised the work critically for intellectual content and approved the final version of the manuscript for publication.

Words in abstract	250
Words in translational relevance section	149
Words in main body	4469

Figures	3
Tables	2

Supplementary notes	1
Supplementary tables	3
Supplementary figures	4

Abstract

Purpose: To explore a prognostic or predictive role of magnetic resonance imaging (MRI) and O-(2-^{18}F-fluoroethyl)-L-tyrosine (^{18}FET) positron emission tomography (PET) parameters for outcome in the randomized multi-center trial ARTE that compared bevacizumab plus radiotherapy with radiotherpay alone in elderly patients with glioblastoma.

Experimental Design: Patients with isocitrate dehydrogenase wild-type glioblastoma aged 65 years or older were included in this post-hoc analysis. Tumor volumetric and apparent diffusion coefficient (ADC) analyses of serial MRI scans from 67 patients and serial ^{18}FET-PET tumor-to-brain intensity ratios (TBR) from 31 patients were analyzed blinded for treatment arm and outcome. Multivariate Cox regression analysis was done to account for established prognostic factors and treatment arm.

Results: Overall survival benefit from bevacizumab plus radiotherapy compared to radiotherapy alone was observed for larger pre-treatment MRI contrast-enhancing tumor (hazard ratio [HR] per cm^3 0.94, 95% confidence interval [CI] 0.89-0.99) and for higher ADC (HR 0.18, CI 0.05-0.66). Higher ^{18}FET-TBR on pre-treatment PET scans was associated with inferior overall survival in both arms. Response assessed by standard MRI-based RANO criteria was associated with overall survival in the bevacizumab plus radiotherapy arm by trend only (p=0.09). High ^{18}FET-TBR of non-contrast-enhancing tumor portions during bevacizumab therapy was associated with inferior overall survival on multivariate analysis (HR 5.97, CI 1.16-30.8).

Conclusion: Large pre-treatment contrast-enhancing tumor mass and higher ADC identify patients who may experience a survival benefit from bevacizumab plus radiotherapy. Persistent ^{18}FET-PET signal of no longer contrast-enhancing tumor after concomitant bevacizumab plus radiotherapy suggests pseudoresponse and predicts poor outcome.

Trial registration: NCT01443676.

Translational Relevance

Response assessment of brain tumor patients exposed to anti-angiogenic therapy remains challenging because reduction of contrast enhancement on MRI may reflect blood brain barrier restoration rather than tumor regression, a phenomenon termed pseudoresponse. The Response Assessment in Neuro-Oncology (RANO) working group supports the use of amino acid PET to monitor non-contrast-enhancing tumor growth in bevacizumab-treated patients based on limited evidence. We herein report the MRI/PET sub-study of a randomized, clinically and molecularly well-annotated multi-center cohort of IDH wild-type glioblastoma patients treated with or without bevacizumab. Our exploratory analyses suggest that larger pre-treatment contrast-enhancing tumor volume and low ^{18}FET intensity of non-contrast-enhancing tumor during bevacizumab treatment may predict survival benefit from bevacizumab plus radiotherapy. MRI response by RANO was only by trend associated with overall survival in bevacizumab-treated patients. Our study supports the use of ^{18}FET

intensity in non-contrast-enhancing tumor to identify pseudoresponse in glioblastoma patients treated with anti-angiogenic agents.

Introduction

Glioblastoma is an invariably fatal disease with a median overall survival in the range of one year (1). The proliferation of hyperplastic, dysfunctional blood vessels is a histological hallmark of glioblastoma (2). Vascular endothelial growth factor A (VEGF), a key driver of angiogenesis in glioblastoma and other cancers, can be targeted with the VEGF-neutralizing antibody bevacizumab (BEV) (3). Definitive FDA approval of BEV for the treatment of recurrent glioblastoma was based on prolonged progression-free survival (PFS) and apparent clinical benefit (4-6). However, randomized clinical trials of BEV in patients with newly diagnosed or recurrent glioblastoma failed to demonstrate prolonged overall survival (6-8).

Pre-treatment magnetic resonance imaging (MRI) parameters, including absence of imaging necrosis or higher apparent diffusion coefficients (ADC), may identify subgroups of patients with overall survival benefit from BEV in recurrent glioblastoma (9-11). How to optimally monitor glioblastoma patients treated with BEV remains a matter of debate, because contrast enhancement on T1-weighted MRI sequences – the key parameter to monitor glioblastoma growth in classical response criteria (12,13) – may decrease within days after implementation of anti-angiogenic therapy and often reflects restoration of blood brain barrier function rather than tumor shrinkage (14-16). This phenomenon has been termed pseudoresponse (17) and may

account for unrecognized disease progression in patients on anti-angiogenic therapy, leading to deferred salvage therapy and potentially even shorter overall survival.

The Response Assessment in Neuro-Oncology (RANO) working group has incorporated clinical parameters and T2-weighted MRI sequences as measures to address the challenges of misleading treatment-induced contrast enhancement dynamics (12). There is however large interobserver variability regarding the time-point of progression by RANO (18) and in BEV-treated patients, response by RANO may not predict overall survival in patients with newly diagnosed (19) or recurrent glioblastoma (20).

Positron emission tomography (PET) utilizing the amino acid tracers O-(2-^{18}F-fluoroethyl)-L-tyrosine (^{18}FET) or (S-^{11}C-methyl)-L-methionine (^{11}C-MET) can be utilized to differentiate viable glioma tissue from treatment-induced changes with high sensitivity and specificity (21). Uncontrolled studies suggest that ^{18}FET-PET may detect tumor progression during anti-angiogenic treatment earlier than MRI (20,22,23). This led the RANO working group to incorporate recommendations for the use of amino acid PET in the response assessment of such patients (24).

The randomized multi-center open label phase II trial ARTE explored the efficacy of BEV as an adjunct to hypofractionated radiotherapy (RT) in elderly patients (> 65 years) with newly diagnosed glioblastoma (25). Here we report associations of serial MRI and ^{18}FET-PET parameters with benefit from BEV plus RT in this clinically and molecularly homogenous, well-annotated cohort of glioblastoma patients.

Patients and methods

Study design

ARTE was a 2:1 randomized phase II clinical trial of hypofractionated RT of 15 x 2.66 = 40 Gy in combination with BEV 10 mg/kg bodyweight administered every two weeks compared to hypofractionated RT alone in elderly (> 65 years) patients with newly diagnosed glioblastoma. Here we analyzed associations of pre-treatment and follow-up imaging parameters by treatment arm with outcome. Patients with isocitrate dehydrogenase (IDH)-mutant glioblastoma or alternative diagnoses by central pathology review were excluded from this analysis. Outcome measures were PFS from randomization and overall survival from histological diagnosis. The ARTE trial and post-hoc translational analyses were approved by the local ethical committee (KEK-ZH No. 2011-0135) and were conducted in accordance with the Declaration of Helsinki and its amendments. All patients gave written informed consent prior to inclusion. The ARTE trial is registered at clinicaltrials.gov (NCT01443676).

Molecular analyses

Analysis of the promoter methylation status of the O^6-methylguanine DNA methyltransferase (*MGMT*) promoter region was done in all patients and a methylated *MGMT* promoter became an exclusion criterion by amendment (November 2013) when it became clear that patients with tumors with a methylated *MGMT* derived

larger benefit from temozolomide monotherapy than from RT alone (26,27). *MGMT* promoter methylation status was determined by methylation-specific PCR (28). *IDH* mutation status was determined by immunohistochemistry (29) or sequencing of *IDH1* and *IDH2*. Genome-wide CpG methylation was determined by 450k array profiling and classified utilizing a publically available tool (www.molecularneuropathology.org) (30). Genomic copy number alterations were derived from methylation arrays and subtypes annotated manually according to prognostic subgroups (31). Gene expression subtypes were determined utilizing the nCounter gene expression platform (NanoString Technologies, Seattle, WA) to assess a custom gene set for subsequent classification based on published centromers (32,33).

MRI and ^{18}FET-PET parameters

Pre-treatment MRI and ^{18}FET-PET were performed post-operatively within 10 days before the start of study treatment, BEV plus RT or RT alone. Follow-up scans were to be acquired 4 weeks after completion of RT (week 7) and at least every three months thereafter until progression. MRI was done according to local investigators' protocols on 1.5 T or 3 T scanners. Gadolinium was used as contrast agent. The slice thickness was at the most 3 mm for any sequences analyzed. There was no centralized specification of echo or repetition times or of field-of-view values. MRI included contrast enhancement and T2 as the minimum set of sequences for volumetric characterization and response assessment. Pre-treatment necrosis was defined as hyperintensity on T2 and hypointensity on T1 located within contrast enhancement.

Diffusion-weighted sequences were expressed by mean ADC in absolute units of $10^{-3}mm^2/s$. ADC_L, the mean of the lower distribution of a double Gaussian model, was also determined. Fractional anisotropy was not reported. Pre-treatment contrast-enhancing and T2 volumes were determined utilizing the Brainlab Elements version 2.6 software (Brainlab, Munich, Germany). Treatment response for MRI sequences was determined according to RANO criteria by measuring perpendicular tumor diameters to yield bidimensional tumor size estimates in mm^2 and taking the clinical course into account (12). Tumor size changes during follow-up were calculated as percent change from pre-treatment scans. Static ^{18}FET-PET scans were acquired 30 to 50 minutes after tracer injection. A standardized imaging acquisition protocol for MRI and PET scans was implemented in all centers participating in the ARTE trial.

Both ADC values and ^{18}FET intensity values were also measured separately for non-enhancing and for enhancing tumor to account for different diffusion properties and passive tracer diffusion (34). Diffusion-weighted MRI and PET images were fused with contrast-enhancing MRI. Non-contrast-enhancing tumor was defined by T2 hyperintensity in the absence of contrast enhancement, i.e. including areas of potential vasogenic edema. PET region-of-interest (ROI) analysis was done outlining the respective tumor compartments on the superimposed MRI and PET images. ROI were determined in two perpendicular planes, each in the slice with the maximum tumor area. For ^{18}FET intensity quantification, tumor-to-brain ratios (TBR) were determined by dividing the mean tumor ROI intensity values on the plane with the largest tumor area on MRI by the mean intensity in a ROI on the plane with the largest cerebellar diameter as the reference (35). Analyses of imaging parameters were done centrally by UR and JW blinded for treatment arm and outcome.

Statistical methods

The Chi-square test was applied to compare categorical variables and the Mann-Whitney-U test was applied for continuous variables. Receiver operator characteristics (ROC) curve analyses utilizing median overall survival to determine prognostic cutoffs were done to segregate patients by continuously scaled imaging parameters. Best response was computed as time-dependent covariate as indicated. Treatment arms and indicated subgroups were compared in exploratory analyses with respect to progression-free survival and overall survival using the log rank test, or univariate and multivariate Cox proportional hazards models incorporating indicated covariates. Age and Karnofsky performance score (KPS) were dichotomized at established cut-offs (age: 71 years or more versus 65-70 years, KPS: <90% versus 90-100%) (25). No correction for multiple testing was done in this exploratory analysis. P-values below 0.05 were considered statistically significant.

Results

Study population

The primary analysis population is detailed in Figure 1. Of 75 patients enrolled, 50 were treated with BEV plus RT and 25 with RT alone. Eight patients were excluded from subsequent analyses, two in the BEV plus RT arm with mutated IDH, one

patient in each arm with an alternative diagnosis on central pathology review, and four patients without pre-treatment MRI available. Longitudinal volumetric analyses of contrast-enhanced and T2-weighted MRI sequences were available from 44 and 23 patients, ADC from 37 and 20 patients, and ^{18}FET-TBR from 19 and 12 patients, in the BEV plus RT and RT arms. Demographic, clinical and molecular characteristics at baseline were balanced between arms, including age, sex, contrast-enhancing tumor volume, Karnofsky performance score (KPS), steroid use, *MGMT* promoter methylation status, genome methylation subtypes and gene expression subtypes in the overall cohort (25), and in the sub-cohorts with available MRI and FET-PET studied here (Table 1, Table S1).

Pre-treatment contrast enhancement and ADC are associated with overall survival benefit from BEV plus RT

ROC curve analyses identified a pre-treatment contrast enhancement cutoff at 3.1 cm^3 that was associated with overall survival by trend in the BEV plus RT arm (Fig. 2A) and at 5.3 cm^3 that segregated patients by overall survival in the RT arm (Fig. 2B). Analyzing contrast-enhancing volumes as continuous variable confirmed that larger pre-treatment contrast-enhancing volume was associated with inferior overall survival in both treatment arms. This association was less pronounced in the BEV plus RT arm than in the RT arm, suggesting that a negative association of contrast enhancement with overall survival is in part abrogated by BEV. Along the same lines, there was an interaction of pre-treatment contrast enhancement with treatment arm indicating

preferential benefit from BEV plus RT in tumors with larger contrast-enhancing volumes (Fig. 2C).

No associations with overall survival in either treatment arm were identified for pre-treatment volumetric analyses of T2-weighted images (Fig. S1A-C), or of fluid attenuated inversion recovery (FLAIR) sequences (not shown). Similar analyses were done utilizing cutoffs of pre-treatment contrast enhancement and T2 volumes with respect to progression-free survival, but we identified no interactions with progression-free survival benefit from BEV plus RT (Note S1, Fig. S2).

We also explored whether imaging necrosis – an MRI surrogate for tumor hypoxia – was associated with overall survival. Necrosis was present in 38 of 67 patients (57%) on pre-treatment MRI scans and presence of any necrosis was associated with inferior outcome (Fig. S3A), but there was no association with benefit from BEV with respect to overall survival (Fig. S3B) or progression-free survival (not shown).

ADC values were analyzed in contrast-enhancing tumor portions and cutoffs to segregate patients by high versus low mean ADC values were defined by ROC curve analyses. In the BEV plus RT arm, pre-treatment ADC values above 1.19 mm^2/s were associated with longer overall survival (Fig. 2D), but no such association was detected in the RT arm (Fig. 2E). There was a marked interaction of pre-treatment ADC with treatment arm indicating preferential overall survival benefit from BEV plus RT in tumors with higher ADC (Fig. 2F). A similar interaction of higher ADC values in contrast-enhancing tumor portions with preferential benefit from BEV plus

RT was also observed with respect to PFS (Fig. S3C).

Pre-treatment ^{18}FET intensity in contrast-enhancing tumor tissue is associated with inferior overall survival independent of treatment

In contrast-enhancing tumor portions, ^{18}FET may enrich due to passive tracer diffusion in addition to active uptake by tumor cells (34), thus requiring the separate analysis of ^{18}FET intensities in contrast-enhancing and non-contrast-enhancing tumor portions. Applying ROC cutoffs of pre-treatment ^{18}FET intensity in contrast-enhancing tumor lesions identified a marked association of higher ^{18}FET-TBR with inferior overall survival in the BEV plus RT arm (Fig. 2G) and by trend in the RT arm (Fig. 2H), but there was no specific overall survival benefit from BEV plus RT among patients with high or low ^{18}FET intensity (Fig. 2I). We compared the association of pre-treatment contrast-enhancing volume, ADC and ^{18}FET intensity TBR with overall survival in a multivariable model that included all three parameters and correction variables for study arm interactions of ADC and contrast-enhancing volumes (Table S2). In this model, high versus low ^{18}FET intensity was negatively associated with overall survival (hazard ratio [HR] 3.54, 95% confidence interval [CI] 1.12-11.16, p=0.031), but not contrast-enhancing volumes (p=0.39) or ADC (p=0.79), suggesting that pre-treatment ^{18}FET intensity in contrast-enhancing tumor portions may reflect prognosis more accurately than MRI-based imaging alone.

In non-contrast-enhancing tumor areas, pre-treatment ^{18}FET intensity TBR were similar to normal brain (not shown), suggesting that pre-treatment T2 hyperintensity

may comprise mostly vasogenic edema and gliosis rather than metabolically active tumor cells. Consequently, no associations with overall survival were identified for pre-treatment ^{18}FET intensity in non-contrast-enhancing tumor portions (not shown). No associations of ^{18}FET intensity TBR with PFS were identified in contrast-enhancing or non-contrast-enhancing tumor areas (not shown), suggesting that the observed association of pre-treatment ^{18}FET PET with overall survival is treatment independent.

Imaging response assessment by RANO is only weakly associated with overall survival in BEV-treated patients

Anti-angiogenic treatment often induces a reduction in contrast enhancement that may occur within days from the initiation of therapy. This phenomenon does not necessarily reflect a reduction in tumor burden but rather restoration of blood brain barrier function (17). One objective of the RANO criteria was to expand criteria for differentiating a definition of imaging response and tumor progression and anti-angiogenic treatment beyond contrast-enhancing tumor, taking clinical and T2-weighted MRI parameters into account (12). In the ARTE trial, response by RANO computed as time-dependent variable was only by trend associated with longer overall survival in the BEV plus RT arm whereas there was a clear segregation by overall survival in the RT arm (Fig. 3A,B). Utilizing the percent changes between best response and pre-treatment value in contrast-enhancing volume estimates, we identified response cutoffs that were associated with overall survival in either treatment arm, albeit the segregation by contrast-enhancing response was less

pronounced in the BEV plus RT arm (cutoff 55% contrast-enhancing volume reduction, median overall survival no response vs response = 9.7 vs 12.9 months, time-dependent p=0.023, Fig. S3D) than in the RT arm (cutoff 10% contrast-enhancing volume reduction, median overall survival no response vs response = 8.9 vs 14.4 months, time-dependent p=0.003, Fig. S3E). No associations with overall survival were observed for percent changes of T2 in either treatment arm (not shown).

^{18}FET-TBR of non-contrast-enhancing lesions is associated with overall survival in BEV-treated patients

^{18}FET-PET was implemented in the ARTE trial to enable detection and monitoring of non-contrast-enhancing tumor burden in areas where anti-angiogenic therapy has led to a tightened blood-brain barrier that prohibits contrast diffusion. Passive tracer diffusion into contrast-enhancing tumor portions (34) implies that the analysis of a metabolic response in either compartment is challenged by effects of BEV on the spatial contrast-enhancing distribution. Comparing ^{18}FET-TBR of non-contrast-enhancing tumor portions to the identical tumor region that was contrast-enhancing before BEV exposure will likely measure a decreased ^{18}FET intensity that may not reflect tumor cell death. As a surrogate for tumor burden and metabolic response to treatment in each compartment, we annotated ^{18}FET-TBR from first follow-up after RT (week 7) until progression in each patient. In patients with decreasing ^{18}FET-TBR at any time during follow-up, we utilized the lowest recorded follow-up value and in patients with increasing ^{18}FET-TBR, we utilized the highest recorded value to define a high versus low ^{18}FET-TBR cutoff by ROC curve analysis. In the BEV plus RT

arm, high ^{18}FET-TBR in non-contrast-enhancing tumor portions during follow-up after RT was associated with inferior overall survival by trend (Fig. 3C), but no such association was identified in the RT arm (Fig. 3D). Vice versa, high ^{18}FET-TBR in contrast-enhancing tumor portions during follow-up after RT was associated with overall survival in the RT arm only (Fig. S4). An example of contrast enhancement, T2 and utilizing ^{18}FET PET is provided in Fig. 3E.

Imaging response by molecular subtypes

We also explored whether distinctive molecular glioblastoma subtypes defined by gene methylation, gene expression or genomic copy number alterations were enriched for response by RANO criteria or for high or low ^{18}FET-TBR in non-contrast-enhancing tumor during BEV therapy. No such association was identified for complete or partial response versus stable disease or no response by RANO (not shown) and likewise, no association of high or low ^{18}FET-TBR in non-contrast-enhancing tumor was identified with gene methylation ($p=0.38$), gene expression ($p=0.37$) or genomic copy number subtypes ($p=0.29$).

Multivariate analyses

We sought to also explore imaging parameters associated with benefit from BEV in a multivariate Cox regression model of overall survival that takes established prognostic factors into account, including age, KPS and steroid intake. Univariate

associations of these parameters with overall survival are summarized in Table S3. Pre-treatment contrast-enhancing tumor and ADC were both associated with overall survival (Table 2). We also identified an association of ADC_L with overall survival in this model (ADC_L HR per 0.1 mm/s^2 = 1.59, 95% CI 1.04-2.43, p=0.033). Follow-up imaging parameters at the first study visit after RT (week 7) were explored in this multivariate model as a clinically relevant paradigm of treatment reevaluation. There was a weak association of a decrease in contrast-enhancing tumor mass with improved overall survival. High non-contrast-enhancing ^{18}FET intensities on a single scan at first follow-up was associated with markedly inferior overall survival, suggesting that pseudoresponse was a negative predictor of overall survival. MGMT promotor methylation status was not associated with overall survival on univariate or multivariate analyses and had no relevant effect on HR determined for ADC or ^{18}FET intensities at baseline or at the first study visit after RT (not shown).

Discussion

The present secondary analyses of the randomized ARTE trial explored MRI- and PET-based parameters for selection and monitoring of patients with newly diagnosed IDH wild-type glioblastoma during BEV therapy.

Pre-treatment MRI parameters including contrast-enhancing tumor and ADC, but not T2 volumes stratified BEV plus RT-treated patients by overall survival and were associated with specific benefit from BEV plus RT compared to RT alone. There was

also a strong association of pre-treatment ^{18}FET intensities in contrast-enhancing tumor with overall survival, but this was not specific for the BEV plus RT arm.

The interaction of larger pre-treatment contrast-enhancing volume with preferential overall survival benefit from BEV plus RT is supported by a less pronounced association of pre-treatment tumor size with overall survival in the BEV plus RT arm than in the RT arm. Similar results by trend have also been reported from the phase III AVAglio trial of BEV in combination with chemoradiotherapy versus chemoradiotherapy alone in newly diagnosed glioblastoma (36). Other factors such as temozolomide treatment and *MGMT* promoter methylation status may have been more important prognostic factors in AVAglio than in ARTE.

Extent of resection was not determined in the ARTE cohort. However, a relevant association of smaller post-operative contrast-enhanced tumor volume with longer overall survival was noted in both treatment arms, supporting maximum safe resection as the standard of care irrespective of whether or not BEV is administered (37).

The phase III European Organization for Research and Treatment of Cancer (EORTC) 26101 trial assessed the efficacy of BEV in combination with lomustine in recurrent glioblastoma (6). Our study expands on post-hoc analyses of this trial in the newly diagnosed setting by confirming an association of baseline imaging necrosis with inferior overall survival (11). A dynamic increase of imaging necrosis during treatment was observed in a small proportion of patients in EORTC 26101 and, irrespective of treatment (11). Similar analyses of outcome by dynamics of necrosis

were not feasible in the ARTE study due to the relatively smaller sample size. In the EORTC 26101 cohort, presence of necrosis also predicted inferior survival of the BEV plus lomustine arm compared with the lomustine alone arm (11), but a similar association of BEV plus RT was not noted in the ARTE cohort.

Our study also supports retrospective studies and reports from uncontrolled clinical trials in recurrent glioblastoma that proposed ADC as a prognostic parameter in patients treated with BEV (9,10,38). As a potential limitation and in contrast to these previous studies, we have however used mean ADC and not a double Gaussian mixed model for most analyses. Nonetheless, the randomized design of our study supports that ADC may be predictive of benefit from bevacizumab rather than a treatment-agnostic prognostic factor.

The rationale for the use of amino acid PET in patients treated with BEV is to identify and monitor viable non-contrast-enhancing tumor portions to account for a commonly observed reduction of contrast enhancement that does not necessarily reflect tumor cell death (17,24). The clinical utility of this rationale was supported by a strong negative association of non-contrast-enhancing ^{18}FET intensity with overall survival specifically in patients treated with BEV plus RT. This association was confirmed on multivariate analyses at first follow-up after radiotherapy, suggesting that amino acid PET may serve as an early marker of pseudoresponse and as a predictor of overall survival benefit during BEV plus RT treatment. By contrast, the similar ^{18}FET intensity of normal brain and non-contrast-enhancing tumor before treatment or post-RT in the RT arm suggest that the majority of hyperintensity on T2-weighted MRI represents vasogenic edema. Our findings support the proposal by the RANO working

group to utilize amino acid PET to monitor tumor growth in BEV-treated glioblastoma patients and complements feasibility studies that have indicated better accuracy of amino acid PET for disease monitoring than conventional MRI in BEV-treated glioma patients (20,22,39-42). However, the small sample size of the PET cohort warrants further validation of amino acid PET as a predictor of overall survival during anti-angiogenic therapy.

The lack of overall survival association of T2 pre-treatment volumes or dynamics in either treatment arm of ARTE is of note given that part of the rationale to include a T2-based definition of progression in the RANO criteria was to account for pseudoresponse to anti-angiogenic therapy (12). Our findings underscore that dynamics of T2 hyperintensity do not generally reflect the disease course, but require careful evaluation in the context of clinical assessments and treatment. For example, a T2 "response" may simply reflect regression of edema in response to BEV, and *vice versa* T2 "progression" may reflect an increase of edema when steroids are weaned, or delayed radiation effects. Along the same lines, response defined by the contrast enhancement- and T2-based RANO criteria were only weakly associated with overall survival in this study and in AVAglio (19).

The lack of overall survival benefit in phase III clinical trials of BEV in combination with standard treatments in newly diagnosed (7,8) and recurrent glioblastoma (6) may be considered at odds with reports of imaging biomarkers that have been proposed to identify patients with presumed overall survival benefit from BEV. If subgroups of patients derive overall survival benefit, other subgroups will experience harm from BEV when the net outcome is neutral.

A possible interpretation may be that the herein reported association of higher ^{18}FET-TBR in non-contrast-enhancing tumor portions with inferior overall survival reflects delayed diagnosis of progression and thus deferred salvage therapy. The considerably smaller proportion of patients in the BEV plus RT arm compared to the RT arm who received any salvage treatment in ARTE (first salvage therapy 25/50 = 50% versus 18/25 = 72%, second salvage therapy 7/50 = 14% versus 14/25 = 56%) (25) supports this explanation. Along the same lines, interobserver bias with respect to the diagnosis of progression by RANO criteria has been reported from several clinical trials with central radiology review, including ARTE (25) and EORTC 26101 (6,18). Albeit not statistically amenable, differences in assessment and outcome between the two phase III clinical trials of BEV in newly diagnosed glioblastoma also support the notion that deferred diagnosis of progression may negatively impact overall survival in patients treated with BEV. The contrast enhancement-based Macdonald criteria (13) in the RTOG 0825 trial and the RANO criteria (12) in the AVAglio trial conveyed HRs for BEV of 1.12 and 0.88, respectively (7,8). However, the fact that the vast majority of patients in the ARTE trial had an unmethylated MGMT promoter questions whether the limited efficacy of temozolomide or lomustine in a recurrent setting would have yielded a clinically relevant difference in overall survival.

Strengths of our study include the thorough annotation of clinical, molecular and imaging parameters. The statistical power was likely further enhanced by the inclusion of only elderly patients, because this patient population is deemed to preferentially benefit from BEV in combination with different chemotherapy regimens based on early uncontrolled trials (5,43,44). Moreover, confounding factors

were reduced by exclusion of patients with IDH mutated glioblastoma, which was defined as a distinct entity in the current World Health Organization (WHO) classification of primary brain tumors based on molecular and clinical features distinct from the majority of glioblastomas that lack IDH mutations (2). Other poor prognostic characteristics of the ARTE cohort include the lack of *MGMT* promoter methylation in the large majority of patients, because patients with methylated *MGMT* promoter were excluded from ARTE by amendment when it became clear that these patients would derive more benefit from temozolomide than from RT (37). That *MGMT* promoter methylation was not prognostic in the ARTE trial is explained by the fact that the patients did not receive first-line temozolomide and that only few patients received alkylating chemotherapy at recurrence.

Limitations of the analysis include its relatively small sample size, particularly in the PET cohort. Although the ARTE trial was designed to include a poor prognosis population – i.e. elderly patients with unmethylated MGMT – the median overall survival of approximately 12 months is considerably longer than expected based on epidemiological studies (1,45). Reasons for this apparent selection of patients with better prognostic traits include that patients were required to be able to travel every other week to receive bevacizumab infusions. The optional participation in the PET study of the ARTE trial required additional traveling and may have aggravated the selection towards patients in a better clinical condition. However, patient characteristics and overall survival were similar in the MRI and PET cohorts, thus arguing against relevant selection bias between these groups.

Another limitation of our study is that BEV is not commonly used in the newly diagnosed setting of the ARTE trial, but mostly at recurrence of glioblastoma. Beyond amino acid PET, the dramatic progress and clinical implementation of advanced MRI technologies warrants the expansion of multimodal imaging for monitoring of glioblastomas, e.g. by MR spectroscopy (46) or perfusion imaging (47). Lastly, the clinical feasibility of machine learning algorithms to define response and progression has been demonstrated in the context of BEV therapy of glioblastoma (18,48), supporting that unbiased approaches may aid in integrating large amounts of data from multimodal imaging in future studies.

In summary, we provide a comprehensive validation of current imaging standards and propose improvements in the context of BEV treatment of glioblastoma. Our study falsifies T2 as a relevant marker of tumor growth during BEV treatment and does not unambiguously support patient selection for BEV treatment based on higher ADC, but supports the preferential use of BEV in patients with larger contrast-enhancing volumes, and the use of amino acid PET to monitor anti-angiogenic treatment (24). Future studies applying these and other parameters prospectively are warranted to improve patient selection and disease monitoring in patients treated with BEV, particularly in the recurrent setting for which BEV has obtained clinical approval in the US and other countries.

Funding

The ARTE trial was supported by a grant from F. Hoffmann-La Roche. HGW was supported by a grant from the University Hospital Zurich.

References

1. Ostrom QT, Cioffi G, Gittleman H, Patil N, Waite K, Kruchko C*, et al.* CBTRUS Statistical Report: Primary Brain and Other Central Nervous System Tumors Diagnosed in the United States in 2012-2016. Neuro Oncol **2019**;21(Supplement_5):v1-v100 doi 10.1093/neuonc/noz150.

2. Louis DN, Perry A, Reifenberger G, von Deimling A, Figarella-Branger D, Cavenee WK*, et al.* The 2016 World Health Organization Classification of Tumors of the Central Nervous System: a summary. Acta Neuropathol **2016**;131(6):803-20 doi 10.1007/s00401-016-1545-1.

3. Presta LG, Chen H, O'Connor SJ, Chisholm V, Meng YG, Krummen L*, et al.* Humanization of an anti-vascular endothelial growth factor monoclonal antibody for the therapy of solid tumors and other disorders. Cancer Res **1997**;57(20):4593-9.

4. Friedman HS, Prados MD, Wen PY, Mikkelsen T, Schiff D, Abrey LE*, et al.* Bevacizumab alone and in combination with irinotecan in recurrent glioblastoma. Journal of clinical oncology : official journal of the American Society of Clinical Oncology **2009**;27(28):4733-40 doi 10.1200/JCO.2008.19.8721.

5. Kreisl TN, Kim L, Moore K, Duic P, Royce C, Stroud I*, et al.* Phase II trial of single-agent bevacizumab followed by bevacizumab plus irinotecan at tumor progression in

recurrent glioblastoma. Journal of clinical oncology : official journal of the American Society of Clinical Oncology **2009**;27(5):740-5 doi 10.1200/JCO.2008.16.3055.

6. Wick W, Gorlia T, Bendszus M, Taphoorn M, Sahm F, Harting I*, et al.* Lomustine and Bevacizumab in Progressive Glioblastoma. The New England journal of medicine **2017**;377(20):1954-63 doi 10.1056/NEJMoa1707358.

7. Chinot OL, Wick W, Mason W, Henriksson R, Saran F, Nishikawa R*, et al.* Bevacizumab plus radiotherapy-temozolomide for newly diagnosed glioblastoma. The New England journal of medicine **2014**;370(8):709-22 doi 10.1056/NEJMoa1308345.

8. Gilbert MR, Dignam JJ, Armstrong TS, Wefel JS, Blumenthal DT, Vogelbaum MA*, et al.* A randomized trial of bevacizumab for newly diagnosed glioblastoma. The New England journal of medicine **2014**;370(8):699-708 doi 10.1056/NEJMoa1308573.

9. Ellingson BM, Sahebjam S, Kim HJ, Pope WB, Harris RJ, Woodworth DC*, et al.* Pretreatment ADC histogram analysis is a predictive imaging biomarker for bevacizumab treatment but not chemotherapy in recurrent glioblastoma. AJNR Am J Neuroradiol **2014**;35(4):673-9 doi 10.3174/ajnr.A3748.

10. Ellingson BM, Gerstner ER, Smits M, Huang RY, Colen R, Abrey LE*, et al.* Diffusion MRI Phenotypes Predict Overall Survival Benefit from Anti-VEGF Monotherapy in Recurrent Glioblastoma: Converging Evidence from Phase II Trials. Clinical cancer research : an official journal of the American Association for Cancer Research **2017**;23(19):5745-56 doi 10.1158/1078-0432.CCR-16-2844.

11. Nowosielski M, Gorlia T, Bromberg JEC, Sahm F, Harting I, Kickingereder P*, et al.* Imaging necrosis during treatment is associated with worse survival in EORTC 26101 study. Neurology **2019**;92(24):e2754-e63 doi 10.1212/WNL.0000000000007643.

12. Wen PY, Macdonald DR, Reardon DA, Cloughesy TF, Sorensen AG, Galanis E*, et al.* Updated response assessment criteria for high-grade gliomas: response assessment in neuro-oncology working group. Journal of clinical oncology : official journal of the American Society of Clinical Oncology **2010**;28(11):1963-72 doi 10.1200/JCO.2009.26.3541.

13. Macdonald DR, Cascino TL, Schold SC, Jr., Cairncross JG. Response criteria for phase II studies of supratentorial malignant glioma. Journal of clinical oncology : official journal of the American Society of Clinical Oncology **1990**;8(7):1277-80 doi 10.1200/JCO.1990.8.7.1277.

14. Batchelor TT, Sorensen AG, di Tomaso E, Zhang WT, Duda DG, Cohen KS*, et al.* AZD2171, a pan-VEGF receptor tyrosine kinase inhibitor, normalizes tumor vasculature and alleviates edema in glioblastoma patients. Cancer cell **2007**;11(1):83-95 doi 10.1016/j.ccr.2006.11.021.

15. Nowosielski M, Wiestler B, Goebel G, Hutterer M, Schlemmer HP, Stockhammer G*, et al.* Progression types after antiangiogenic therapy are related to outcome in recurrent glioblastoma. Neurology **2014**;82(19):1684-92 doi 10.1212/WNL.0000000000000402.

16. Reardon DA, Ballman KV, Buckner JC, Chang SM, Ellingson BM. Impact of imaging measurements on response assessment in glioblastoma clinical trials. Neuro Oncol **2014**;16 Suppl 7:vii24-35 doi 10.1093/neuonc/nou286.

17. Brandsma D, van den Bent MJ. Pseudoprogression and pseudoresponse in the treatment of gliomas. Current opinion in neurology **2009**;22(6):633-8 doi 10.1097/WCO.0b013e328332363e.

18. Kickingereder P, Isensee F, Tursunova I, Petersen J, Neuberger U, Bonekamp D*, et al.* Automated quantitative tumour response assessment of MRI in neuro-oncology

with artificial neural networks: a multicentre, retrospective study. The Lancet Oncology **2019**;20(5):728-40 doi 10.1016/S1470-2045(19)30098-1.

19. Ellingson BM, Abrey LE, Garcia J, Chinot O, Wick W, Saran F*, et al.* Post-chemoradiation volumetric response predicts survival in newly diagnosed glioblastoma treated with radiation, temozolomide, and bevacizumab or placebo. Neuro Oncol **2018**;20(11):1525-35 doi 10.1093/neuonc/noy064.

20. Galldiks N, Dunkl V, Ceccon G, Tscherpel C, Stoffels G, Law I*, et al.* Early treatment response evaluation using FET PET compared to MRI in glioblastoma patients at first progression treated with bevacizumab plus lomustine. Eur J Nucl Med Mol Imaging **2018**;45(13):2377-86 doi 10.1007/s00259-018-4082-4.

21. de Zwart PL, van Dijken BR, Holtman GA, Stormezand GN, Dierckx RA, van Laar PJ*, et al.* Diagnostic accuracy of positron emission tomography tracers for the differentiation of tumor progression from treatment-related changes in high-grade glioma: a systematic review and meta-analysis. J Nucl Med **2019** doi 10.2967/jnumed.119.233809.

22. Galldiks N, Rapp M, Stoffels G, Fink GR, Shah NJ, Coenen HH*, et al.* Response assessment of bevacizumab in patients with recurrent malignant glioma using [18F]Fluoroethyl-L-tyrosine PET in comparison to MRI. Eur J Nucl Med Mol Imaging **2013**;40(1):22-33 doi 10.1007/s00259-012-2251-4.

23. Hutterer M, Nowosielski M, Putzer D, Waitz D, Tinkhauser G, Kostron H*, et al.* O-(2-18F-fluoroethyl)-L-tyrosine PET predicts failure of antiangiogenic treatment in patients with recurrent high-grade glioma. J Nucl Med **2011**;52(6):856-64 doi 10.2967/jnumed.110.086645.

24. Albert NL, Weller M, Suchorska B, Galldiks N, Soffietti R, Kim MM*, et al.* Response Assessment in Neuro-Oncology working group and European Association

for Neuro-Oncology recommendations for the clinical use of PET imaging in gliomas. Neuro Oncol **2016**;18(9):1199-208 doi 10.1093/neuonc/now058.

25. Wirsching HG, Tabatabai G, Roelcke U, Hottinger AF, Jorger F, Schmid A*, et al.* Bevacizumab plus hypofractionated radiotherapy versus radiotherapy alone in elderly patients with glioblastoma: the randomized, open-label, phase II ARTE trial. Ann Oncol **2018**;29(6):1423-30 doi 10.1093/annonc/mdy120.

26. Malmstrom A, Gronberg BH, Marosi C, Stupp R, Frappaz D, Schultz H*, et al.* Temozolomide versus standard 6-week radiotherapy versus hypofractionated radiotherapy in patients older than 60 years with glioblastoma: the Nordic randomised, phase 3 trial. The Lancet Oncology **2012**;13(9):916-26 doi 10.1016/s1470-2045(12)70265-6.

27. Wick W, Platten M, Meisner C, Felsberg J, Tabatabai G, Simon M*, et al.* Temozolomide chemotherapy alone versus radiotherapy alone for malignant astrocytoma in the elderly: the NOA-08 randomised, phase 3 trial. The Lancet Oncology **2012**;13(7):707-15 doi 10.1016/s1470-2045(12)70164-x.

28. Felsberg J, Rapp M, Loeser S, Fimmers R, Stummer W, Goeppert M*, et al.* Prognostic significance of molecular markers and extent of resection in primary glioblastoma patients. Clinical cancer research : an official journal of the American Association for Cancer Research **2009**;15(21):6683-93 doi 10.1158/1078-0432.CCR-08-2801.

29. Capper D, Zentgraf H, Balss J, Hartmann C, von Deimling A. Monoclonal antibody specific for IDH1 R132H mutation. Acta neuropathologica **2009**;118(5):599-601 doi 10.1007/s00401-009-0595-z.

30. Capper D, Jones DTW, Sill M, Hovestadt V, Schrimpf D, Sturm D*, et al.* DNA methylation-based classification of central nervous system tumours. Nature **2018**;555(7697):469-74 doi 10.1038/nature26000.

31. Cimino PJ, Zager M, McFerrin L, Wirsching HG, Bolouri H, Hentschel B*, et al.* Multidimensional scaling of diffuse gliomas: application to the 2016 World Health Organization classification system with prognostically relevant molecular subtype discovery. Acta neuropathologica communications **2017**;5(1):39 doi 10.1186/s40478-017-0443-7.

32. Sandmann T, Bourgon R, Garcia J, Li C, Cloughesy T, Chinot OL*, et al.* Patients With Proneural Glioblastoma May Derive Overall Survival Benefit From the Addition of Bevacizumab to First-Line Radiotherapy and Temozolomide: Retrospective Analysis of the AVAglio Trial. J Clin Oncol **2015** doi 10.1200/JCO.2015.61.5005.

33. Verhaak RG, Hoadley KA, Purdom E, Wang V, Qi Y, Wilkerson MD*, et al.* Integrated genomic analysis identifies clinically relevant subtypes of glioblastoma characterized by abnormalities in PDGFRA, IDH1, EGFR, and NF1. Cancer cell **2010**;17(1):98-110 doi 10.1016/j.ccr.2009.12.020.

34. Hutterer M, Nowosielski M, Putzer D, Jansen NL, Seiz M, Schocke M*, et al.* [18F]-fluoro-ethyl-L-tyrosine PET: a valuable diagnostic tool in neuro-oncology, but not all that glitters is glioma. Neuro Oncol **2013**;15(3):341-51 doi 10.1093/neuonc/nos300.

35. Roelcke U, Wyss MT, Nowosielski M, Ruda R, Roth P, Hofer S*, et al.* Amino acid positron emission tomography to monitor chemotherapy response and predict seizure control and progression-free survival in WHO grade II gliomas. Neuro Oncol **2016**;18(5):744-51 doi 10.1093/neuonc/nov282.

36. Ellingson BM, Abrey LE, Nelson SJ, Kaufmann TJ, Garcia J, Chinot O*, et al.* Validation of postoperative residual contrast-enhancing tumor volume as an independent prognostic factor for overall survival in newly diagnosed glioblastoma. Neuro Oncol **2018**;20(9):1240-50 doi 10.1093/neuonc/noy053.

37. Weller M, van den Bent M, Tonn JC, Stupp R, Preusser M, Cohen-Jonathan-Moyal E*, et al.* European Association for Neuro-Oncology (EANO) guideline on the diagnosis and treatment of adult astrocytic and oligodendroglial gliomas. The Lancet Oncology **2017**;18(6):e315-e29 doi 10.1016/S1470-2045(17)30194-8.

38. Pope WB, Qiao XJ, Kim HJ, Lai A, Nghiemphu P, Xue X*, et al.* Apparent diffusion coefficient histogram analysis stratifies progression-free and overall survival in patients with recurrent GBM treated with bevacizumab: a multi-center study. Journal of neuro-oncology **2012**;108(3):491-8 doi 10.1007/s11060-012-0847-y.

39. Harris RJ, Cloughesy TF, Pope WB, Nghiemphu PL, Lai A, Zaw T*, et al.* 18F-FDOPA and 18F-FLT positron emission tomography parametric response maps predict response in recurrent malignant gliomas treated with bevacizumab. Neuro Oncol **2012**;14(8):1079-89 doi 10.1093/neuonc/nos141.

40. Galldiks N, Rapp M, Stoffels G, Dunkl V, Sabel M, Langen KJ. Earlier diagnosis of progressive disease during bevacizumab treatment using O-(2-18F-fluorethyl)-L-tyrosine positron emission tomography in comparison with magnetic resonance imaging. Mol Imaging **2013**;12(5):273-6.

41. Deuschl C, Moenninghoff C, Goericke S, Kirchner J, Koppen S, Binse I*, et al.* Response assessment of bevacizumab therapy in GBM with integrated 11C-MET-PET/MRI: a feasibility study. Eur J Nucl Med Mol Imaging **2017**;44(8):1285-95 doi 10.1007/s00259-017-3661-0.

42. George E, Kijewski MF, Dubey S, Belanger AP, Reardon DA, Wen PY*, et al.* Voxel-Wise Analysis of Fluoroethyltyrosine PET and MRI in the Assessment of Recurrent Glioblastoma During Antiangiogenic Therapy. AJR Am J Roentgenol **2018**;211(6):1342-7 doi 10.2214/AJR.18.19988.

43. Nghiemphu PL, Liu W, Lee Y, Than T, Graham C, Lai A*, et al.* Bevacizumab and chemotherapy for recurrent glioblastoma: a single-institution experience. Neurology **2009**;72(14):1217-22 doi 10.1212/01.wnl.0000345668.03039.90.

44. Lai A, Tran A, Nghiemphu PL, Pope WB, Solis OE, Selch M*, et al.* Phase II study of bevacizumab plus temozolomide during and after radiation therapy for patients with newly diagnosed glioblastoma multiforme. Journal of clinical oncology : official journal of the American Society of Clinical Oncology **2011**;29(2):142-8 doi 10.1200/JCO.2010.30.2729.

45. Gramatzki D, Dehler S, Rushing EJ, Zaugg K, Hofer S, Yonekawa Y*, et al.* Glioblastoma in the Canton of Zurich, Switzerland revisited: 2005 to 2009. Cancer **2016**;122(14):2206-15 doi 10.1002/cncr.30023.

46. Hattingen E, Jurcoane A, Bahr O, Rieger J, Magerkurth J, Anti S*, et al.* Bevacizumab impairs oxidative energy metabolism and shows antitumoral effects in recurrent glioblastomas: a 31P/1H MRSI and quantitative magnetic resonance imaging study. Neuro Oncol **2011**;13(12):1349-63 doi 10.1093/neuonc/nor132.

47. Kickingereder P, Radbruch A, Burth S, Wick A, Heiland S, Schlemmer HP*, et al.* MR Perfusion-derived Hemodynamic Parametric Response Mapping of Bevacizumab Efficacy in Recurrent Glioblastoma. Radiology **2016**;279(2):542-52 doi 10.1148/radiol.2015151172.

48. Chang K, Zhang B, Guo X, Zong M, Rahman R, Sanchez D*, et al.* Multimodal imaging patterns predict survival in recurrent glioblastoma patients treated with bevacizumab. Neuro Oncol **2016**;18(12):1680-7 doi 10.1093/neuonc/now086.

Table 1. Patient characteristics at baseline.

	BEV plus RT N=44	RT N=23	p
Age, years			
Median	70	69	
Range	65-87	65-79	0.62
Sex, N (%)			
Male	25 (57)	11 (48)	
Female	19 (43)	12 (52)	0.48
Tumor volume, cm^3 *			
Median	3.5	1.1	
Range	0.0-54.1	0.5-40.0	0.35
KPS, N (%)			
90-100	22 (50)	15 (65)	
70-80	18 (41)	6 (26)	
60	4 (9)	2 (9)	0.46
Steroids, N (%)			
Yes	21 (49)	11 (48)	
No	22 (51)	12 (52)	0.94
No data	1	0	
***MGMT* promoter, N (%)**			
Methylated	8 (19)	6 (27)	
Unmethylated	34 (81)	16 (73)	0.45
No data	2	1	
Gene methylation class, N (%)			
Receptor tyrosine kinase I	11 (31)	5 (28)	
Receptor tyrosine kinase II	15 (43)	8 (44)	
Mesenchymal	8 (23)	5 (28)	
Oncogene *MYCN*-driven	1 (3)	0 (0)	0.88
No data	9	5	
Gene expression subtype, N (%)			
Proneural	8 (25)	6 (38)	
Classical	11 (34)	8 (50)	
Mesenchymal	13 (41)	2 (12)	0.14
No data	12	7	

* defined as contrast-enhancing lesions on T1-weighted images; Abbreviations: CL, classical; KPS, Karnofsky performance score.

Table 2. Multivariate analysis of predictors of inferior overall survival.

	HR and 95% CI	**p**
Model		
Study arm: BEV plus RT vs. RT	0.78 (0.44-1.37)	0.39
Age: 65-70 years vs. >70 years	0.46 (0.27-0.78)	0.004
KPS: 90-100% vs. 60-80%	0.62 (0.35-1.09)	0.098
Steroids at study entry: no vs. yes	0.86 (0.56-1.42)	0.56
Imaging parameters*		
Baseline		
contrast enhancement (per cm^3)	1.07 (1.01-1.13)	0.017
ADC (per 0.1 mm/s^2)	1.43 (1.04-1.98)	0.030
First follow-up (post-RT, Week 7)		
contrast enhancement (per 10% response)	0.97 (0.95-0.99)	0.021
^{18}FET intensity in non-contrast-enhancing tumor portions (high vs low)$^+$	5.97 (1.16-30.8)	0.033

* adjusted for interaction with study arm and tested as additional single variables; $^+$cutoffs defined by ROC curve analyses; univariate analyses are summarized in Table S3.

Figure legends

Figure 1. Study population. Abbreviations: ADC, apparent diffusion coefficients; BEV plus RT, bevacizumab in combination with hypofractionated radiotherapy; CE, contrast enhancement on T1-weighted MRI sequences; ^{18}FET-PET, O-(2-^{18}F-fluoroethyl)-L-tyrosine positron emission tomography; IDH, isocitrate dehydrogenase; MRI, magnetic resonance imaging; RANO, response assessment in neuro-oncology working group criteria; RT, radiotherapy alone.

Figure 2. Overall survival by pre-treatment MRI parameters. Overall survival was analyzed by contrast-enhancing volumes (CE-T1) (A-C), ADC values (D-F) and ^{18}FET intensity (G-I). Cutoffs for Kaplan Meier curves were determined by ROC curve analyses and depict patients in the BEV plus RT arm (A, D, G) and in the RT arm (B, E, H). Hazard ratios of indicated imaging parameters were determined for the entire cohort, interaction testing with treatment (interact BEV) and treatment arms utilizing the Cox proportional hazards method (C, F, I). Contrast-enhancing tumor volume was analyzed as continuously scaled variable depicting the hazard per cm^3, ADC and ^{18}FET intensity values were dichotomized by ROC cutoffs.

Figure 3. Overall survival by MRI and PET response. A, B, Overall survival by best response classified as response versus no response at any timepoint until progression determined by the RANO criteria in the BEV plus RT arm (A) and in the RT alone arm (B). C, D, Overall survival by best metabolic response classified as high versus low ^{18}FET-TBR of non-contrast-enhancing tumor portions at any timepoint post treatment until progression in the BEV plus RT arm (C) and in the RT

alone arm (D); ^{18}FET-TBR cut-offs were determined by ROC curve analysis; overall survival of patients with high versus low ^{18}FET-TBR was compared by the Cox proportional hazards method computing best response as a time-dependent variable. E, example of indicated imaging parameters before treatment and at progression; ^{18}FET-PET confirms tumor progression within non-CE-T1, T2 hyperintense regions; CE-T1, contrast enhancement on T1-weighted MRI sequences.

Supplementary Material

Note S1 – Associations of pre-treatment parameters with progression-free survival

Larger contrast-enhancing tumor volume was associated with shorter progression-free survival in the BEV plus RT arm (median progression-free survival CE-T1 high vs. low = 6.4 vs. 8.6 months, log rank p=0.034, Fig. S2A), but not in the RT arm (median progression-free survival CE-T1 high vs. low = 5.4 vs. 5.8 months, p=0.47, Fig. S2B). Utilizing univariate Cox regression to also explore CE-T1 tumor volumes as continuous variable yielded similar results, but identified no prognostic interaction with bevacizumab (Fig. S2C). Similarly, larger pre-treatment T2 volumes were associated with shorter progression-free survival in the BEV plus RT arm (median progression-free survival T2 high vs. low = 6.1 vs. 8.6 months, log rank p=0.003, Fig. S2D), but not in the RT arm (median progression-free survival T2 high vs. low = 4.2 vs. 5.6 months, p=0.72, Fig. S2E) and likewise no interaction with bevacizumab was determined (Fig. S2F).

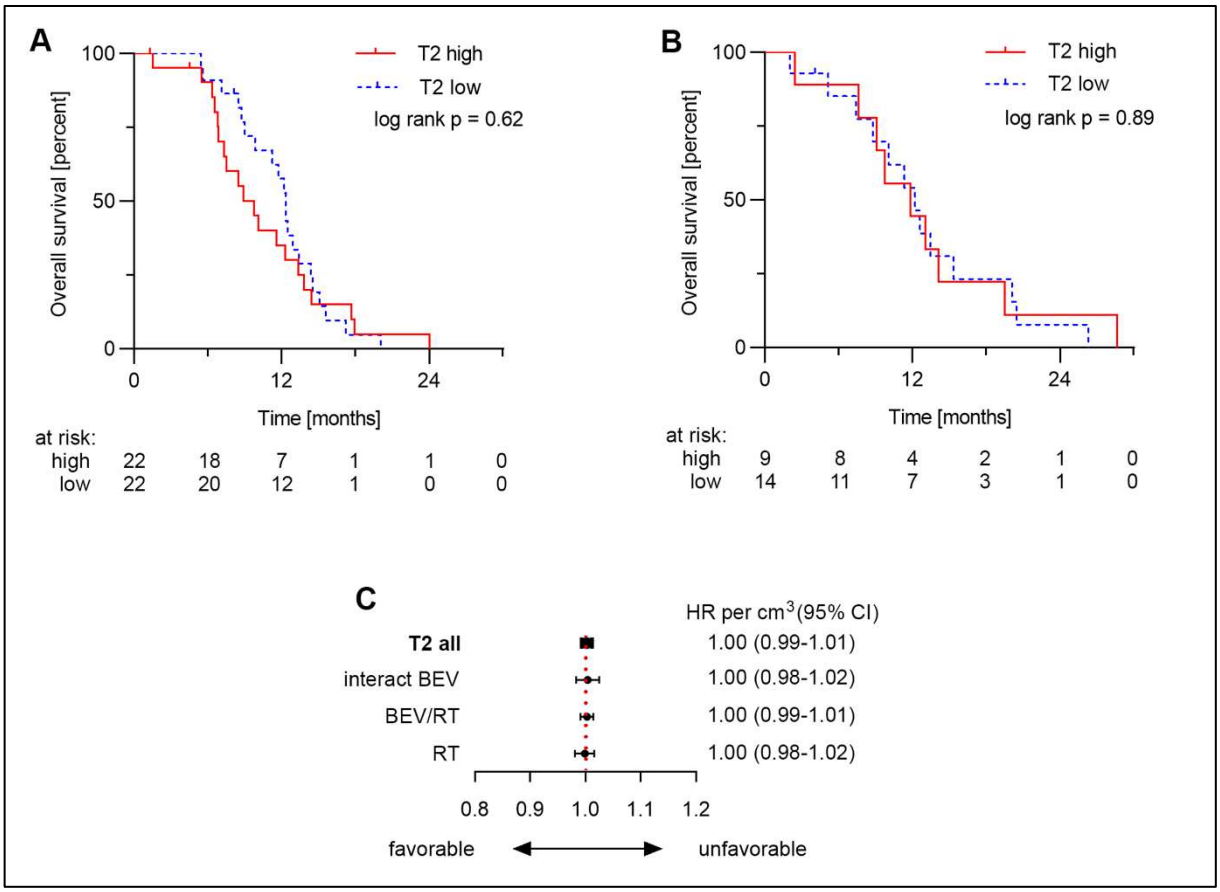

Figure S1. Overall survival by pre-treatment T2-weighted MRI volumes. A, B, Cutoffs for Kaplan Meier curves were determined by receiver operator characteristics (ROC) curve analyses in the BEV plus RT arm (A) and in the RT arm (B). C, Hazard ratios were determined for the entire cohort, interaction testing with treatment (interact BEV) and treatment subgroups utilizing the Cox proportional hazards method. T2 was analyzed as continuously scaled variable depicting the hazard per cm^3.

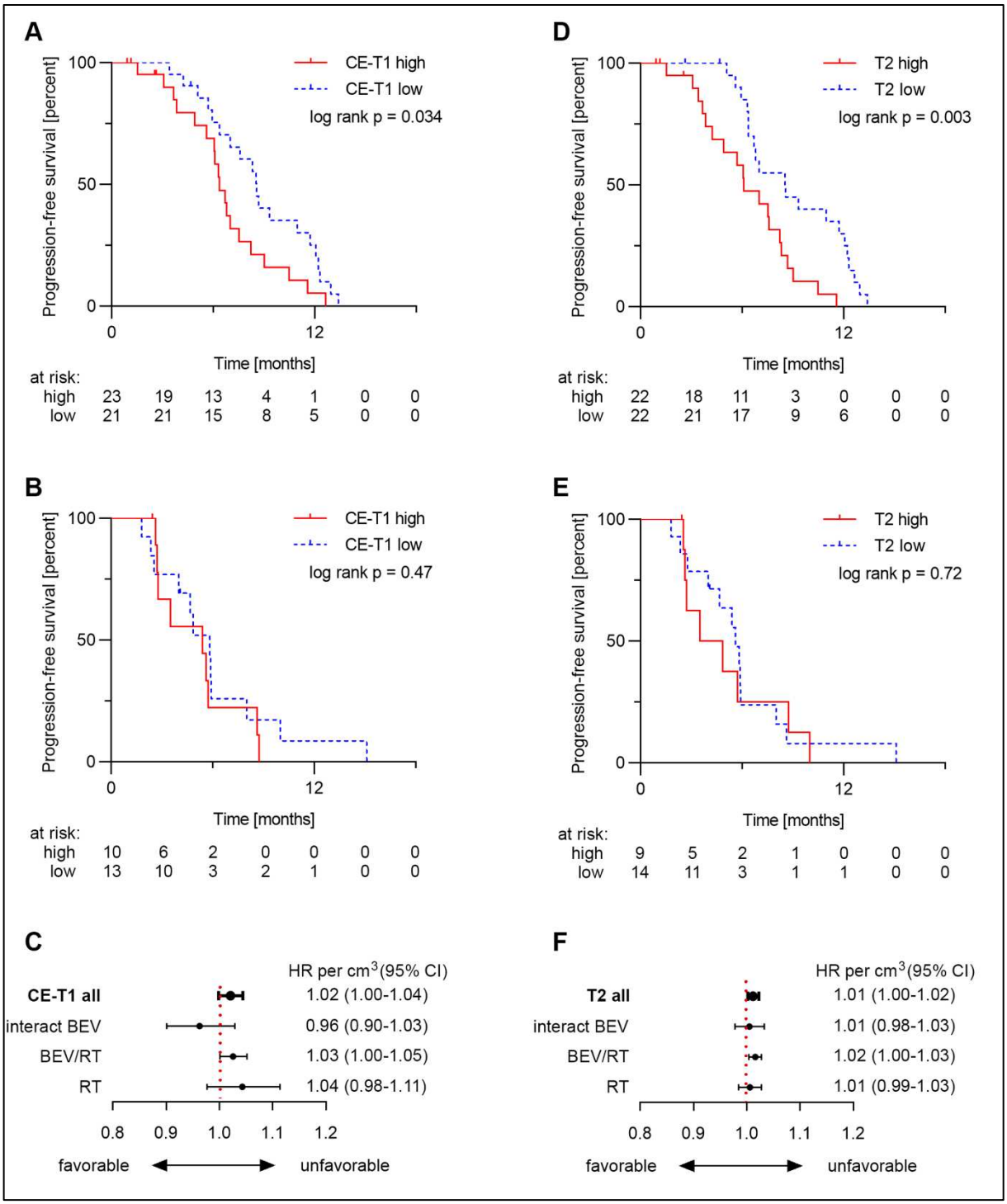

Figure S2. Progression-free survival by pre-treatment MRI parameters. progression-free survival was analyzed by CE-T1 volumes (A-C) and by T2 volumes (D-F). Cutoffs for Kaplan Meier curves were determined by receiver operator characteristics (ROC) curve analyses and depict patients in the BEV plus RT arm (A, D) and in the RT arm (B, E). Hazard ratios of indicated continuously scaled imaging parameters were determined for the entire cohort, interaction testing with treatment (interact BEV) and treatment subgroups utilizing the Cox proportional hazards method and are expressed as hazard ratio per cm^3 (C, F).

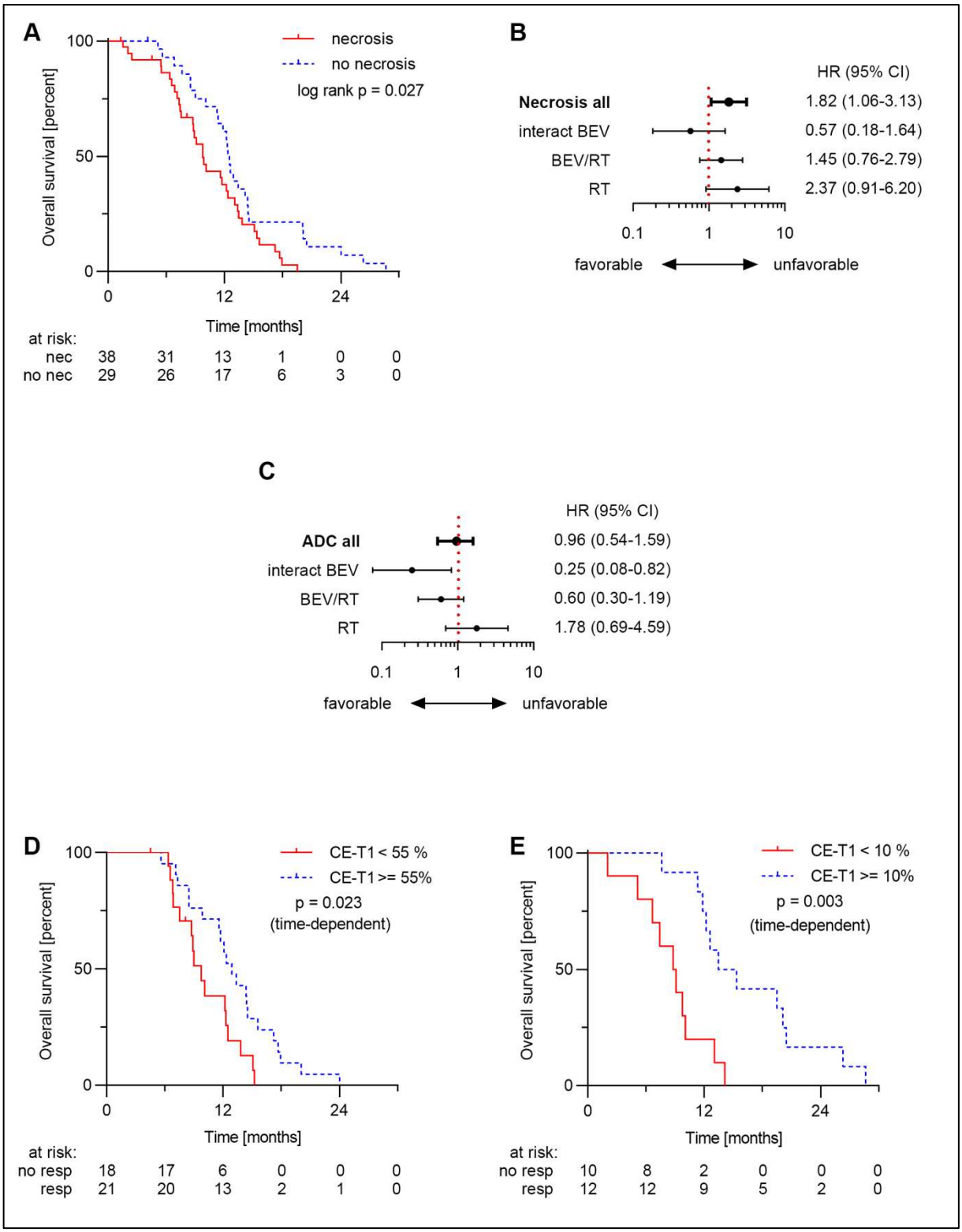

Figure S3. Associations of pre-treatment and response parameters with progression-free survival and overall survival. A, overall survival of the entire study cohort stratified by presence or absence of necrosis on T1 weighted sequences of pre-treatment MRI scans. B, Hazard ratios of continuously scaled pre-treatment necrosis volumes on T1 weighted MRI sequences were determined with respect to overall survival for the entire cohort, interaction testing with treatment (interact BEV) and treatment subgroups utilizing the Cox proportional

hazards method and are expressed as hazard ratio per cm^3. C, Hazard ratios of high versus low ADC values were determined with respect to progression-free survival for the entire cohort, interaction testing with treatment (interact BEV) and treatment subgroups utilizing the Cox proportional hazards method. ADC values were dichotomized by ROC curve analysis. D, E, overall survival by best contrast enhancement response classified as response versus no response at any timepoint until progression in the BEV plus RT arm (D) and in the RT arm (E). Percent response cutoffs were determined by receiver operator characteristics curve analyses and were compared by the Cox proportional hazards method computing best response as a time-dependent variable.

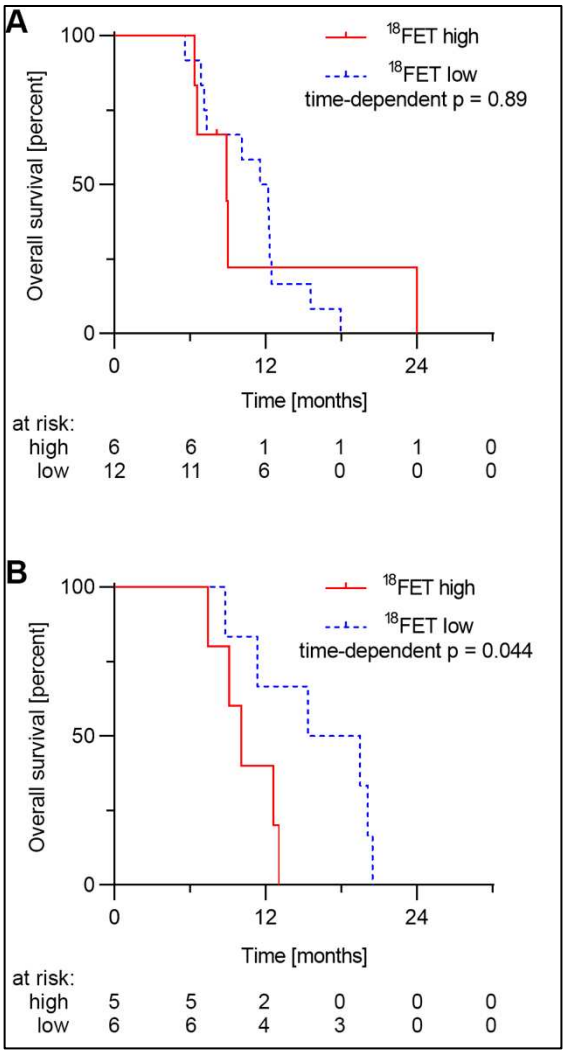

Figure S4. Overall survival by ^{18}FET intensity of CE-T1 tumor portions during treatment. Overall survival was analyzed in the BEV plus RT arm (A) and in the RT arm (B). Cutoffs in each treatment arm were determined by ROC curve analyses of 18FET tumor-to-brain intensity ratios from first follow-up after RT (week 7) until progression utilizing the lowest recorded value in patients with decreasing post-RT 18FET TBR and the highest value in patients with increasing values. For survival analyses, group assignments were computed as time-dependent variables.

Table S1. Patient characteristics of the ADC and FET-PET cohorts.

	ADC cohort N=57			FET-PET cohort N=31		
	BEV plus RT N=37	RT N=20	p	BEV plus RT N=19	RT N=12	p
Age at diagnosis, years						
Median	70	70		70	69	
Range	65-83	65-77	0.93	65-87	66-74	0.80
Gender, N (%)						
Male	25 (68)	12 (60)				
Female	12 (32)	8 (40)	0.57			
Tumor volume at study entry, cm^3						
Median	2.9	1.7		3.3	2.2	
Range	0.0-54.1	0.5-25.4	0.54	0.0-54.1	0.5-25.4	0.70
KPS at study entry, N (%)						
90-100	17 (46)	12 (60)		11 (58)	4 (33)	
70-80	17 (46)	6 (30)		6 (32)	8 (67)	
60	3 (8)	2 (10)	0.64	2 (10)	0 (0)	0.65
Steroids at study entry, N (%)						
Yes	18 (50)	9 (45)		8 (42)	4 (33)	
No	18 (50)	11 (55)	0.72	11 (58)	8 (67)	0.63
No data	1	0		0	0	
***MGMT* promoter status, N (%)**						
Methylated	8 (22)	5 (25)		3 (16)	3 (25)	
Unmethylated	28 (78)	15 (75)	0.81	16 (84)	9 (75)	0.53
No data	1	0		0	0	
Gene methylation subtype, N (%)						
Receptor Tyrosine Kinase I	10 (32)	4 (27)		4 (27)	1 (10)	
Receptor Tyrosine Kinase II	14 (45)	7 (46)		8 (53)	6 (60)	
Mesenchymal Oncogene *MYCN*-driven	6 (19) 1 (3)	4 (27) 0 (0)	0.84	2 (13) 1 (7)	3 (30) 0 (0)	0.80
No data	6	5		4	2	
Gene expression subtype, N (%)						
Proneural	8 (30)	5 (42)		0 (0)	1 (17)	
Classical	10 (37)	5 (42)		6 (50)	4 (66)	
Mesenchymal	9 (33)	2 (16)	0.54	6 (50)	1 (17)	0.30
No data	10	8		7	6	

Table S2. Multivariable analysis of associations of pre-treatment imaging parameters with overall survival.

	HR (95% CI)	**p**
Contrast enhancement (per cm^3) *	1.05 (0.95-1.16)	0.79
ADC in contrast-enhancing tumor portion: high versus low *	1.27 (0.22-7.32)	0.39
^{18}FET TBR in contrast-enhancing tumor portion: high versus low	3.54 (1.12-11.16)	0.032

* corrected for interactions with study arm; univariate analyses are given in Figures 2C, 2F and 2I.

Table S3. Univariate analysis of associations with overall survival of variables analyzed in the multivariate model in Table 2.

	HR and 95% CI	**p**
Study arm: BEV plus RT vs. RT	1.08 (0.65-1.78)	0.77
Age: 65-70 years vs. >70 years	0.51 (0.31-0.82)	0.006
KPS: 90-100% vs. 60-80%	0.46 (0.27-0.78)	0.004
Steroids at study entry: no vs. yes	0.63 (0.39-1.02)	0.059

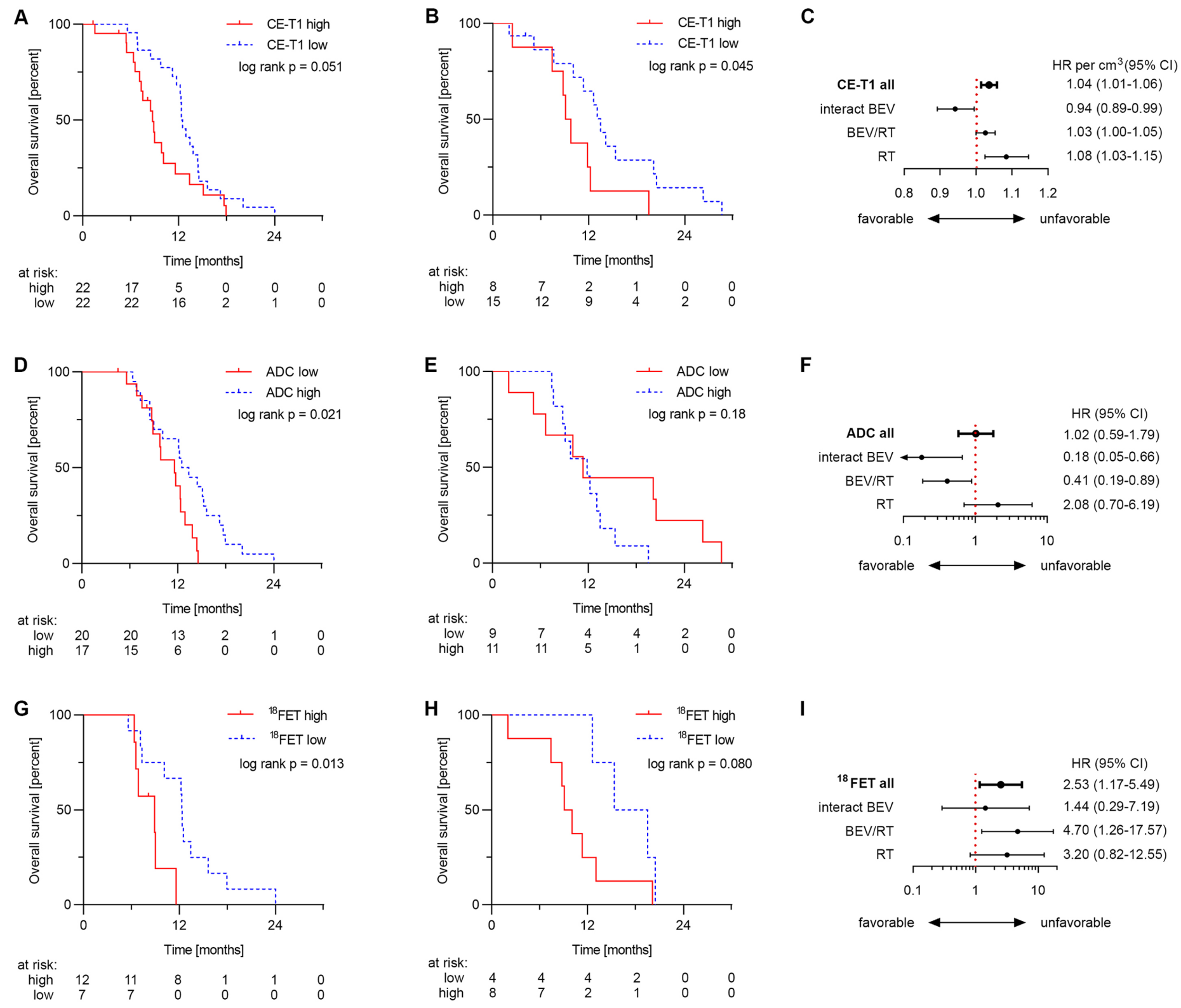
A
Overall survival [percent]
CE-T1 high
CE-T1 low
log rank p = 0.051
Time [months]
at risk:
high 22 17 5 0 0 0
low 22 22 16 2 1 0
B
CE-T1 high
CE-T1 low
log rank p = 0.045
Time [months]
at risk:
high 8 7 2 1 0 0
low 15 12 9 4 2 0
C
HR per cm3 (95% CI)
CE-T1 all 1.04 (1.01-1.06)
interact BEV 0.94 (0.89-0.99)
BEV/RT 1.03 (1.00-1.05)
RT 1.08 (1.03-1.15)
favorable
unfavorable
D
ADC low
ADC high
log rank p = 0.021
Time [months]
at risk:
low 20 20 13 2 1 0
high 17 15 6 0 0 0
E
ADC low
ADC high
log rank p = 0.18
Time [months]
at risk:
low 9 7 4 4 2 0
high 11 11 5 1 0 0
F
HR (95% CI)
ADC all 1.02 (0.59-1.79)
interact BEV 0.18 (0.05-0.66)
BEV/RT 0.41 (0.19-0.89)
RT 2.08 (0.70-6.19)
favorable
unfavorable
G
18FET high
18FET low
log rank p = 0.013
Time [months]
at risk:
high 12 11 8 1 1 0
low 7 7 0 0 0 0
H
18FET high
18FET low
log rank p = 0.080
Time [months]
at risk:
low 4 4 4 2 0 0
high 8 7 2 1 0 0
I
HR (95% CI)
18FET all 2.53 (1.17-5.49)
interact BEV 1.44 (0.29-7.19)
BEV/RT 4.70 (1.26-17.57)
RT 3.20 (0.82-12.55)
favorable
unfavorable

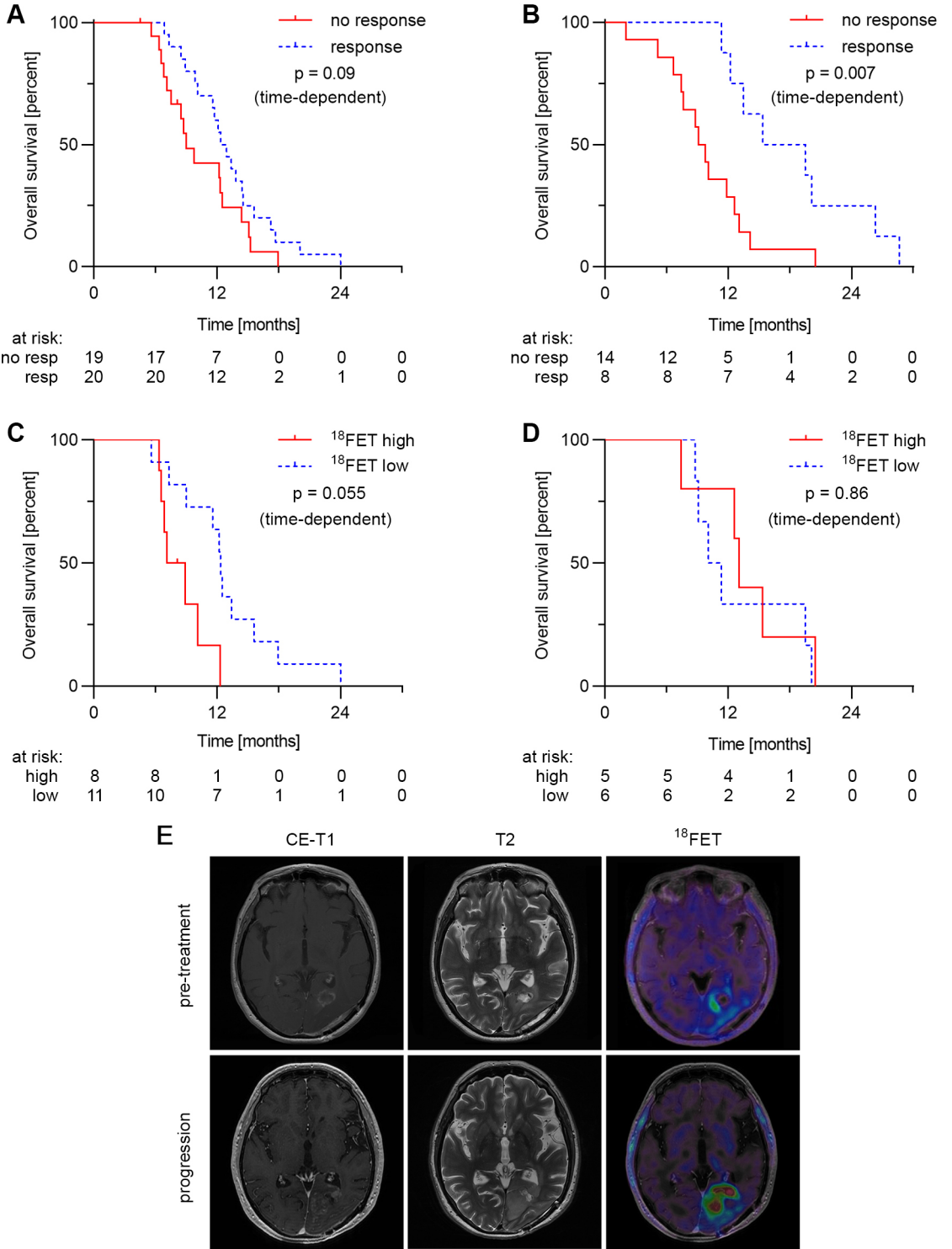
A
100
50
0
Overall survival [percent]
no response
response
p = 0.09
(time-dependent)
0
12
24
Time [months]
at risk:
no resp 19 17 7 0 0 0
resp 20 20 12 2 1 0
B
100
50
0
Overall survival [percent]
no response
response
p = 0.007
(time-dependent)
0
12
24
Time [months]
at risk:
no resp 14 12 5 1 0 0
resp 8 8 7 4 2 0
C
100
50
0
Overall survival [percent]
18FET high
18FET low
p = 0.055
(time-dependent)
0
12
24
Time [months]
at risk:
high 8 8 1 0 0 0
low 11 10 7 1 1 0
D
100
50
0
Overall survival [percent]
18FET high
18FET low
p = 0.86
(time-dependent)
0
12
24
Time [months]
at risk:
high 5 5 4 1 0 0
low 6 6 2 2 0 0
E
CE-T1
T2
18FET
pre-treatment
progression

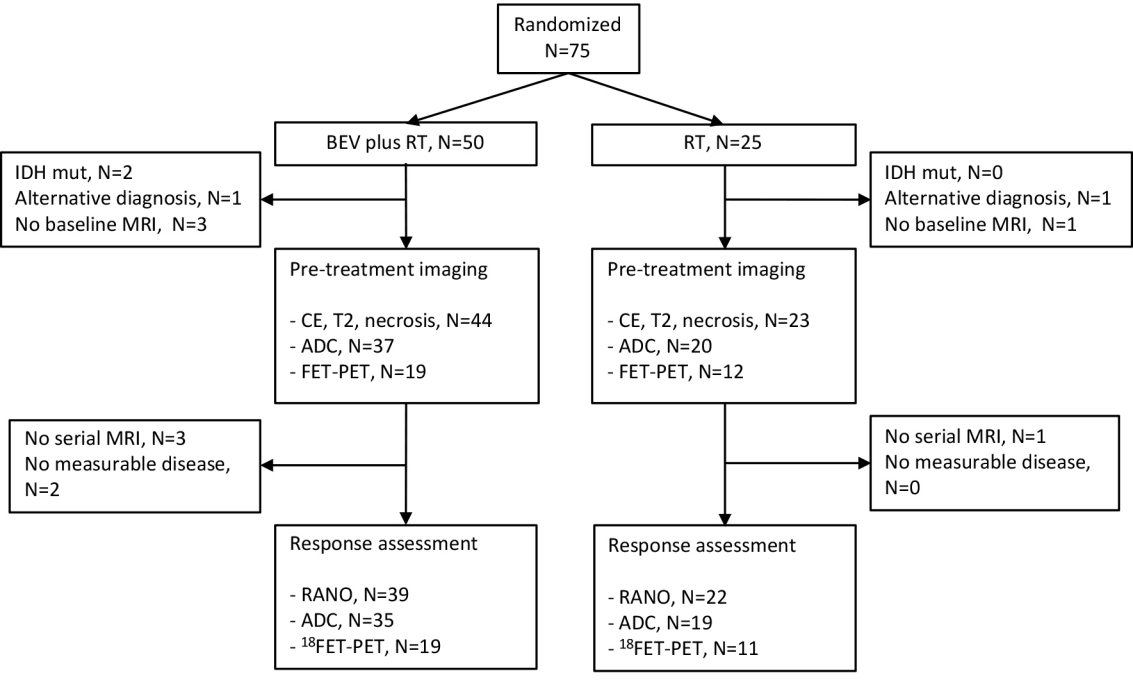
Randomized
N=75
BEV plus RT, N=50
RT, N=25
IDH mut, N=2
Alternative diagnosis, N=1
No baseline MRI, N=3
IDH mut, N=0
Alternative diagnosis, N=1
No baseline MRI, N=1
Pre-treatment imaging
- CE, T2, necrosis, N=44
- ADC, N=37
- FET-PET, N=19
Pre-treatment imaging
- CE, T2, necrosis, N=23
- ADC, N=20
- FET-PET, N=12
No serial MRI, N=3
No measurable disease, N=2
No serial MRI, N=1
No measurable disease, N=0
Response assessment
- RANO, N=39
- ADC, N=35
- 18FET-PET, N=19
Response assessment
- RANO, N=22
- ADC, N=19
- 18FET-PET, N=11